15th Canadian Masonry Symposium
Ottawa, Canada
June 2-5, 2025

Numerical Seismic Assessment of Strengthened Masonry Piers through a Novel 3D Nonlinear Macroelement

Christian Salvatori[i], Gabriele Guerrini[ii], Alessandro Galasco[iii], and Andrea Penna[iv]

ABSTRACT

The seismic vulnerability of unreinforced masonry (URM) structures and their extensive presence worldwide has driven significant efforts in the assessment and retrofit of existing buildings and in the design and detailing of new construction. The seismic performance of existing URM buildings is often compromised by local overturning mechanisms, as these constructions were predominantly conceived without consideration of horizontal forces. However, even if local failure is prevented through structural interventions or adequate construction details, the building might still result inadequate to withstand the in-plane seismic demand. To improve the performance of URM structures, retrofitted solutions involving material with significant tensile strength, such as Fabric-Reinforced Cementitious Matrices (FRCM), Composite-Reinforced Mortars (CRM), Near-Surface-Mounted (NSM) bars, steel or timber exoskeletons, applied to one or both sides of the masonry walls, are commonly employed.

This paper presents a novel three-dimensional equivalent-frame macroelement that extends a previous two-dimensional formulation and resorts to a computationally efficient axial-flexural integration to simulate the nonlinear static and dynamic behavior of URM panels with a limited number of degrees of freedom. In particular, the versatility of the proposed formulation allows incorporating additional lumped and distributed reinforcement into the macroelement, and explicitly modeling several reinforcing and strengthening layouts. The capability of the resulting macroelement formulation in reproducing lateral strength and stiffness, hysteretic cycles, and displacement capacity of masonry panels, is finally validated against experimental outcomes.

KEYWORDS

Equivalent-frame modeling, masonry structures, nonlinear three-dimensional macroelement, seismic analysis, strengthening interventions.

[i] Post-doctoral Research, Department of Civil Engineering and Architecture, University of Pavia, Pavia, Italy, christian.salvatori@unipv.it
[ii] Assistant Professor, Department of Civil Engineering and Architecture, University of Pavia, Pavia, Italy, Gabriele.guerrini@unipv.it
[iii] Research Consultant, Department of Civil Engineering and Architecture, University of Pavia, Pavia, Italy, alessandro.galasco@unipv.it
[iv] Full Professor, Department of Civil Engineering and Architecture, University of Pavia, Pavia, Italy, andrea.penna@unipv.it

INTRODUCTION

Unreinforced masonry (URM) structures constitute a significant portion of the global building stock, particularly in historical centers and rural areas. However, these buildings typically exhibit pronounced seismic vulnerability due to their inherent material weaknesses and lack of adequate provisions to withstand horizontal actions, which might result in local out-of-plane failure mechanisms. Even after addressing out-of-plane response issues and promoting a global three-dimensional behavior, the seismic performance under horizontal excitations might still remain inadequate. Consequently, the research community has focused substantial efforts on developing effective and efficient strategies for strengthening existing URM structures and designing new buildings, including the adoption of reinforced and confined masonry techniques.

Among the available strengthening approaches, single- or double-sided jacketing with Fiber-Reinforced Polymer (FRP) stripes or sheets initially replaced the traditional reinforced plaster method, mitigating its undesired increase in panel weight and stiffness. However, the advent of Composite-Reinforced Mortars (CRM) and Fabric-Reinforced Cementitious Matrices (FRCM) systems provided enhanced chemical and physical compatibility with masonry substrates, making them more suitable alternatives to FRP applications ([1],[2]). In more recent years, interest has increased in improving the seismic performance of existing URM structures while ensuring that retrofit solutions remain cost-effective, sustainable, lightweight, and reversible. This has led researchers to explore the potential of steel ([3]) and timber ([4]) exoskeletons as viable strengthening strategies, especially when integrated with thermal insulation enhancement.

As national and international building codes and guidelines lack standardized prescriptions to effectively account for strengthening intervention on existing masonry elements, the need to reliably simulate experimental response through numerical models has gained increased interest. Consequently, this paper proposes a novel three-dimensional macroelement formulation developed to incorporate the bi-axial contribution of lumped and distributed reinforcing and strengthening layouts into the static and dynamic response of masonry panels.

The formulation builds upon the macroelement developed by Penna et al. ([5]), whose analytical description of the in-plane axial-flexural response, combined with its entirely mechanical basis, has proven highly effective and efficient for static and dynamic analyses of URM structures. The original macroelement has been continuously revised and improved over the years, by correcting some limitations ([6]) and by enhancing its capabilities ([7]). However, its formulation has always been restricted to the in-plane response of unstrengthened masonry members, with extensions to strengthened solutions achieved only by manually adjusting material mechanical properties ([8]), as suggested by the Italian building code ([9],[10]). Also, recent developments have tried to simulate reinforced members ([11]), yet requiring additional elements that need to be accurately calibrated and might significantly affect the computational demand of the analysis.

Following the approach by Vanin et al. ([12]), the original formulation is enhanced by introducing an additional mid-height interface, which allows to capture the correct elastic axial and flexural stiffness simultaneously, without needing to adjust the elastic modulus manually or requiring the iterative algorithm proposed by Bracchi et al. ([6]). To allow 3D response to be modeled, the interfaces are implemented through a stripe or a full fiber discretization, favoring the computational efficiency on the one hand, as stresses are analytically integrated along each stripe, or the numerical versatility on the other hand, as it accommodates more refined constitutive laws. The assembling algorithm employed for the sectional discretization proves suitable for explicitly accounting for additional materials, as lumped or distributed

reinforcement, enforcing their collaboration with the macroelement interfaces through kinematic compatibility constraints.

The capabilities of the proposed macroelement are proved through the simulation of two experimental quasi-static in-plane cyclic shear-compression tests ([4],[13]). In the first case, a masonry pier is investigated in an unstrengthened configuration. In the second one, the same pier is retrofitted using a timber frame and oriented strand boards (OSBs), mechanically connected to the masonry. The vertical posts of the timber frame are explicitly modeled through additional lumped elements, whose bi-axial collaboration with the macroelement interfaces is enforced via kinematic compatibility relationships. Conversely, the shear improvement provided by the OSB panels is implicitly accounted for by enhancing the mechanical properties of masonry. An explicit representation of their contribution will be integrated into the shear formulation in future developments.

THREE-DIMENSIONAL MACROELEMENT FORMULATION

Masonry panels

The need for efficiently and effectively simulating the response of URM structures has driven the development of the equivalent-frame strategy as a viable alternative for the more accurate, yet computational demanding, finite or discrete element methods. By employing nonlinear macroelements, this approach significantly reduces the number of degrees of freedom of the model, focusing on the average behavior of entire masonry panels, rather than on the local response of masonry material.

The two-node three-dimensional macroelement proposed in this paper stems from the formulation of Penna et al. ([5]). In fact, the macroelement proposed in [5] proved particularly suitable for the static and dynamic analyses of masonry structures, as it allows decoupling flexural and shear responses of masonry panels through internal degrees of freedom, while reproducing the corresponding failure mechanisms with a reasonable compromise between accuracy of results and computational effort.

The macroelement comprises five parts (Figure 1a): three zero-height interfaces (*i* and *j* at the panel extremities, and *e* at mid-height) where the axial-flexural response is concentrated, and two central bodies (*A* and *B*) susceptible to shear deformations only. The kinematics of the macroelement is described by eighteen local degrees of freedom (Figure 1a). Six DOFs are located at the two extremities, involving the three displacements and rotations in the three-dimensional space. Additionally, each central body includes a vertical displacement and two rotations about the in-plane and out-of-plane local axes. Similarly to the macroelement of Penna et al. ([5]), the internal DOFs ensure equilibrium at the element level and define the relative generalized displacements associated with the bi-axial flexural response of the interfaces (Figure 1b) and with the shear and torsional responses of the central bodies.

As proposed by Vanin et al. ([12]), the mid-height interface serves as a release for the kinematics of the macroelement, overcoming the limitation of the elastic stiffness of the original two-dimensional formulation ([5]) without requiring an iterative algorithm ([6]). Indeed, each nonlinear interface acts as an integration point that, according to the Gauss-Lobatto integration scheme, allows the exact integration of a third-order polynomial expression. This corresponds to a second-order polynomial curvature profile, which can describe the elastic solution of a beam subjected to concentrated and uniformly distributed loads. In this context, integration lengths of 1/6 and 2/3 of the height of the panel are assigned to the end- and central interfaces, respectively.

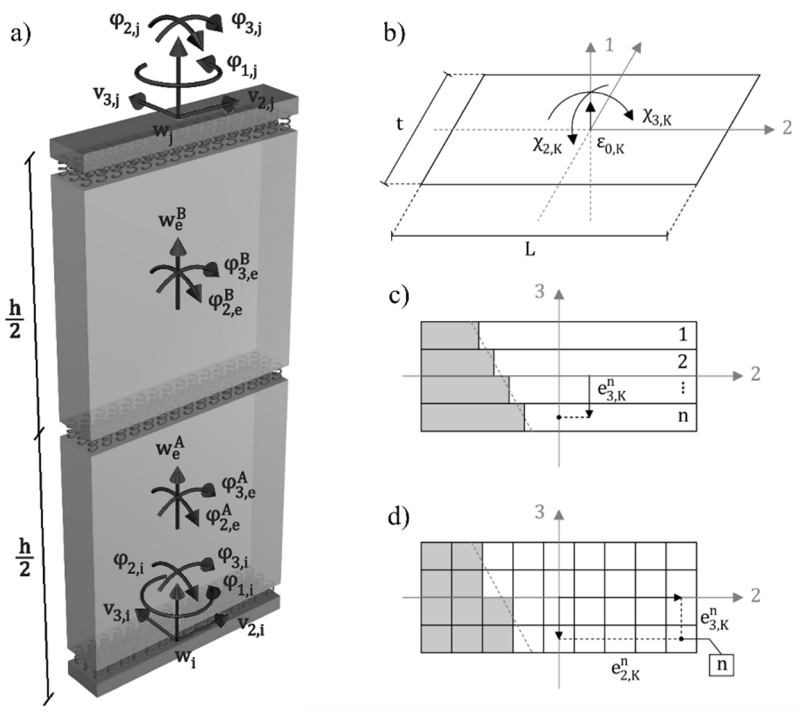

Figure 1: (a) Local degrees of freedom of the three-dimensional macroelement, (b) interface degrees of freedom, (c) stripe and (d) full fiber discretization of the cross-section.

The bi-axial response of the interfaces under flexure and axial load is obtained either by a stripe (Figure 1c) or full fiber discretization (Figure 1d). In the first case, the internal forces related to the K^{th} interface are computed by numerically integrating the response of n analytical two-dimensional homogeneous stripes along the thickness t of the macroelement ([12]), accounting for their out-of-plane eccentricity ($e^n_{3,K}$) with respect to the centroid of the cross-section. The axial deformation $\varepsilon^n_{0,K}$ and the in-plane curvature χ^n_K of the n^{th} stripe, are expressed as:

$$(1)\quad \varepsilon^n_{0,K} = \varepsilon_{0,K} + \chi_{2,K} e^n_{3,K} \qquad \chi^n_K = \chi_{3,K}$$

This procedure favors the computational time, as the in-plane response of each stripe is analytically obtained following the method described by Penna et al. ([5]). In this context, an elastic-perfectly plastic material model, with stiffness degradation and recentering behavior, is adopted in compression (Figure 2a). Furthermore, an elasto-fragile tensile behavior is implemented to introduce an additional level of detail without affecting the computational efficiency of the formulation.

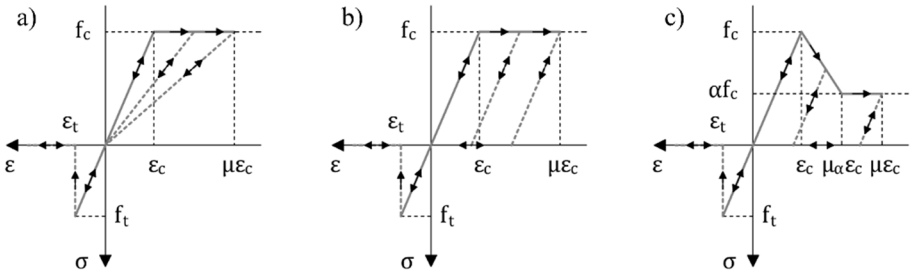

Figure 2: Interface constitutive laws: (a) Penna et al. [5], (b) Bracchi et al. [6] and (c) multilinear material models.

In the second case, the interfaces are instead discretized in a series of uniaxial fibers (Figure 1c), numerically integrated along the two principal directions of the macroelement cross-section. The axial deformation of the n^{th} fiber of the K^{th} interface is computed as reported in Eq. 2:

$$(2)\quad \varepsilon_K^n = \varepsilon_{0,K} + \chi_{2,K} e_{3,K}^n - \chi_{3,K} e_{2,K}^n$$

As no analytical integration is required, more refined constitutive laws can be assigned to the individual fibers. However, the computational time might increase. In this context, the constitutive laws reported in Figure 2b and Figure 2c are provided. Notably, an analytical formulation for the no-tension version of the model depicted in Figure 2b has already been derived by Bracchi et al. ([6]) as an improvement for the original recentering behavior ([5]). Indeed, a parallel-elastic unloading branch allows to better account for energy dissipation and residual displacements. For this reason, the model reported in Figure 2b will be analytically integrated and made available for stripe-discretized interfaces in future developments.

As previously described, the central bodies of the macroelement accommodate the shear and torsional responses. In the current implementation, those responses are considered independent among each other and in the two principal directions, with constant deformation distributions assuming no loads applied between end nodes. The torsional response is maintained linear-elastic, as it is typically of minor concern for masonry members. On the other hand, the shear response is governed by the Gambarotta and Lagomarsino ([14],[15]) continuum model for masonry, macroscopically integrated to align with the macroelement formulation ([5]).

Reinforcement and strengthening

Reinforcement and strengthening of masonry elements are common techniques to improve the seismic performance of unreinforced buildings. In this context, materials with significant tensile strength are applied to or embedded in the original masonry elements, overcoming one of the main deficiencies of the material.

The proposed macroelement allows to explicitly account for the bi-axial contribution of surface and lumped strengthening/reinforcement solutions. Indeed, additional analytical stripes or fibers with different mechanical properties can be easily introduced within the interfaces (Figure 3), ensuring compatibility by forcing the kinematic constraints reported in Eq. 1 and Eq. 2, respectively, which correspond to imposing an a-priori linear profile for the deformations.

Single- or double-sided surface layers can be modeled according to a stripe or fiber discretization and are typically used to simulate jacketing applications ([16]). In the first case, an analytical no-compression elasto-fragile tensile relationship (Figure 4a) adds to the constitutive models discussed in Figure 2. In the cases of a fiber discretization of the jacketing layers or of lumped strengthening/reinforcement, an elastoplastic model is also proposed (Figure 4b,c) based on the well-established J2 plasticity theory, which offers optional isotropic (Figure 4b) or kinematic (Figure 4c) hardening.

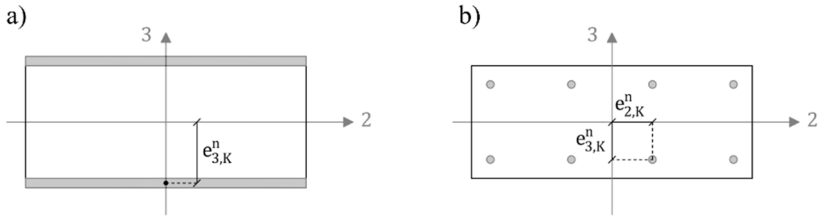

Figure 3: Strengthening and reinforcement on the K^{th} interface: (a) surface layers and (b) lumped elements.

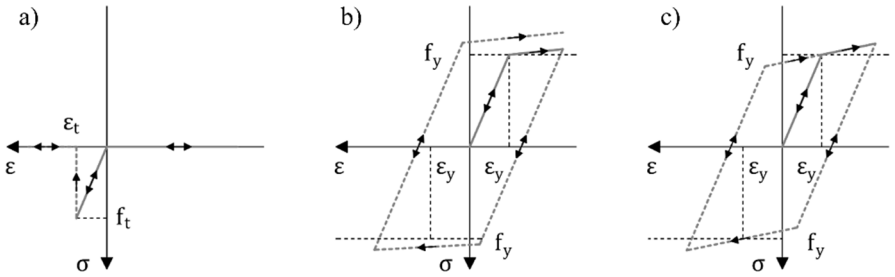

Figure 4: Interface constitutive laws for strengthening/reinforcement solutions: (a) no-compression elasto-fragile tensile relationship; elastoplastic material models with (b) isotropic and (c) kinematic hardening.

As previously discussed, the bi-axial response is automatically accounted for by enforcing kinematic constraints on the deformation profile of the interfaces. On the other hand, the shear contribution of the additional elements is not directly considered in the current formulation.

VALIDATION OF THE MACROELEMENT FORMULATION

The proposed macroelement is used to simulate the experimental response of two single-wythe calcium silicate (CS) masonry piers tested during an experimental campaign ([17]) conducted at the EUCENTRE Foundation and University of Pavia facilities in Italy. The first pier consists of bare masonry, whereas the second one is strengthened with an innovative solution based on timber elements. The specimens are subjected to a quasi-static in-plane cyclic shear-compression test ([4]).

Specimens and testing protocol

The specimens present identical geometry and mechanical properties, consisting of CS masonry piers measuring 2.70 m in height, 2.00 m in length, and 0.10 m in thickness (Figure 5). The strengthened configuration is characterized by a timber frame linked to the masonry underneath, to the top reinforced concrete (RC) beam, and to the RC footing through steel connections (Figure 5b). The timber frame comprises vertical posts and horizontal nogging elements. The vertical posts are fastened to the top and bottom sill plates and to the top and bottom RC elements through specific tie-down anchorages designed to yield before reaching the timber strength (Figure 5b). To enhance the in-plane shear strength and stiffness of the masonry panel, 18-mm-thick oriented strand boards (OSBs) are nailed to the frame. Additional details on the configuration of the retrofitting system can be found in [4].

The mechanical properties of the CS masonry were determined through a series of characterization tests conducted at the DICAr Laboratory of the University of Pavia ([18]). More specifically, the masonry exhibited a Young's modulus $E = 6593$ MPa, with tensile and compressive strengths $f_t = 0.28$ MPa and $f_c = 10.1$ MPa, respectively. Cohesion and friction coefficient resulted in $f_{v0} = 0.62$ MPa and $\mu = 0.71$, while the masonry density was found to be $\rho = 1837$ kg/m³. Finally, CS bricks resulted in tensile and compressive strengths of $f_{bt} = 2.5$ MPa and $f_{bc} = 19.8$ MPa, respectively.

The specimens were subjected to in-plane cyclic shear-compression tests with increasing target displacements through a horizontal servo-hydraulic actuator, while two vertical actuators maintained a constant axial load corresponding to an average stress of about $\sigma_0 = 0.5$ MPa at the pier top and ensured double-curvature boundary conditions. A restraining system prevented the out-of-plane displacements of the piers. Three cycles per displacement increment were performed to investigate stiffness and strength degradation, and the specimens were tested up to severe damage conditions.

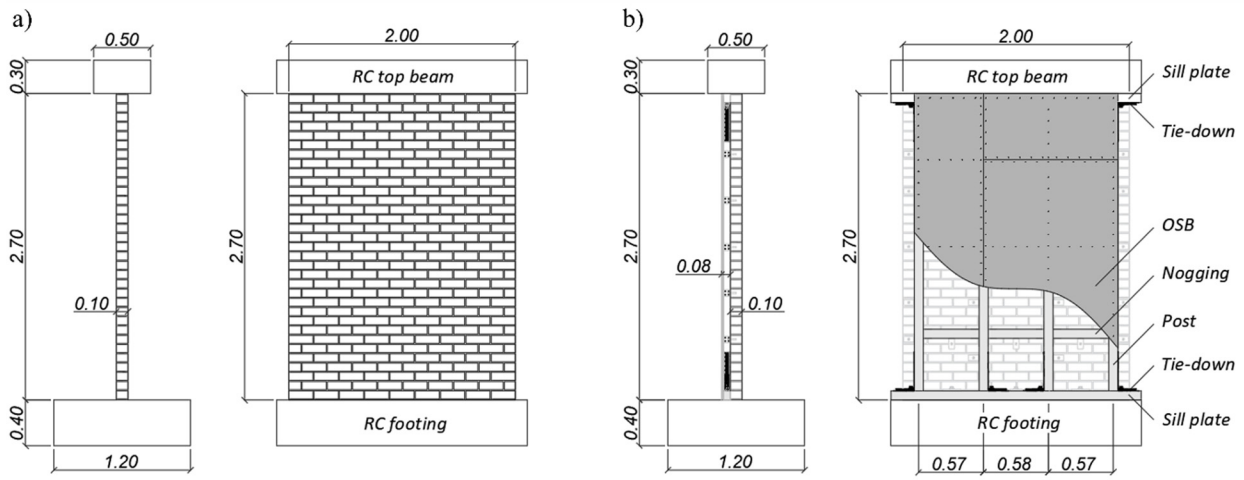

Figure 5: Geometry and details of the tested masonry piers: (a) bare and (b) retrofitted configurations ([4],[13]).

Numerical modeling

The two masonry piers are modeled with their actual geometrical dimensions and by imposing double-fixed boundary conditions. The mechanical properties assigned to the masonry material entirely reflect the experimental values obtained after the characterization campaign ([18]). Only the compressive strength is reduced to 85% when using the elastic-perfectly plastic idealizations: indeed, the constitutive models reported in Figure 2a and Figure 2b cannot reproduce the post-peak softening response of the material. On the contrary, when the model depicted in Figure 2c is used, no modifications are necessary; consequently, the original compressive strength of masonry can be assigned. In this case, a residual strength $\alpha f_c = 0.4\, f_c$ is set at $\mu_\alpha \varepsilon_c = 0.35\%$ of deformation. Finally, the shear modulus is conventionally taken as $G = 0.3E$.

The axial-flexural contribution of the strengthening solution is explicitly modeled by incorporating lumped elements with an elastic-perfectly plastic response (Figure 3b,c) within the macroelement interfaces. More specifically, four additional elements are introduced at the end-interfaces to simulate the tie-down anchorages (Figure 5). Equivalent Young's modulus, cross-sectional area, and yielding stress of these lumped elements are computed to replicate their actual axial stiffness and tensile strength ([4]) (namely 126000 kN/m and 12.8 kN, respectively), based on the integration lengths assigned to the end-interfaces. The strengthening is irrelevant in the central interface, as no relative rotations are expected in double-fixed boundary conditions.

Unlike the bi-axial response, the shear strength of the piers is described as the minimum force resulting from the failure criteria provided. In this context, the shear sliding ($V_{u,s}$) on the cracked length (L') and the stair-stepped diagonal cracking ($V_{u,d}$) are implemented, consistently with the prescription of the Italian building codes for masonry with regular texture ([9],[10]):

$$(3)\quad \begin{cases} V_{u,s} = L'\, t\, f_{v0} + L\, t\, \mu\, \sigma_0 \le f_{v0,lim}\, L'\, t \\ V_{u,d} = L\, t\, \left(\frac{f_{v0}}{1+\mu \tan\phi} + \frac{\mu}{1+\mu \tan\phi}\, \sigma_0\right) \le \frac{L\, t}{2.3}\, f_{bt} \sqrt{1 + \frac{\sigma_0}{f_{bt}}} \end{cases}$$

where $\varphi = 0.7$ is the interlocking coefficient, function of the height and overlapping length of the units ([18]), whereas $f_{v0,lim}$ is a limit due to tensile failure of masonry units, typically expressed in terms of their compressive strength. Since the tensile strength of bricks is directly available from the characterization campaign ([18]), $f_{v0,lim} = f_{bt}$ is assumed.

The shear strength enhancement due to the OSB panels is implicitly accounted for by assigning equivalent cohesion and friction coefficients, following the methodology described in [19] and [20]. In this case, only the stair-stepped diagonal cracking criterion is activated, as the strengthening solution inhibits shear sliding failure mechanisms. Finally, parameters $Gc_t = 5$ and $\beta = 0.5$ are given to the Gambarotta and Lagomarsino ([14],[15]) shear model.

The numerical analyses are performed by imposing the constant vertical force acting at the top of the specimen (i.e., 101.45 kN) and a horizontal displacement history consistent with the testing protocol, in both amplitude and number of cycles.

Numerical results and comparison

Numerical results are compared to the experimental data in terms of hysteresis cycles and failure mechanisms. Hysteresis cycles are expressed as horizontal displacements at the top of the piers against the base shear restoring forces. Additionally, drift ratios are also reported, namely the horizontal displacements normalized with respect to the height of the piers.

The numerical failure mode of the bare pier aligns closely with the experimental observations (Figure 6). In fact, the pier initially exhibited a rocking response, followed by a sudden strength drop due to the onset of a shear-sliding failure mechanism at approximately 0.20% drift ratio. Hysteresis cycles show numerical results in good agreement with the experimental outcomes in terms of elastic stiffness, lateral strength, and energy dissipation. Average discrepancies of 5.5% and 3.9% are obtained for peak and residual lateral strength, respectively. Notably, the peak strength of the numerical model is controlled by the limitation due to failure of CS units ($f_{v0,lim}$), making the results very sensitive to this parameter.

Figure 6a, Figure 6b, and Figure 6c represent the numerical results by assigning the masonry material the constitutive law depicted in Figure 2a, Figure 2b, and Figure 2c, respectively. As can be seen, no differences arise, as the masonry compressive strength is not reached during the imposed displacement history. In previous studies ([16]) it was also pointed out that stripe and full fiber discretizations with the material model of Figure 2a yield almost overlapping results, with minor discrepancies due to the approximations involved in the analytical integration procedure ([5]).

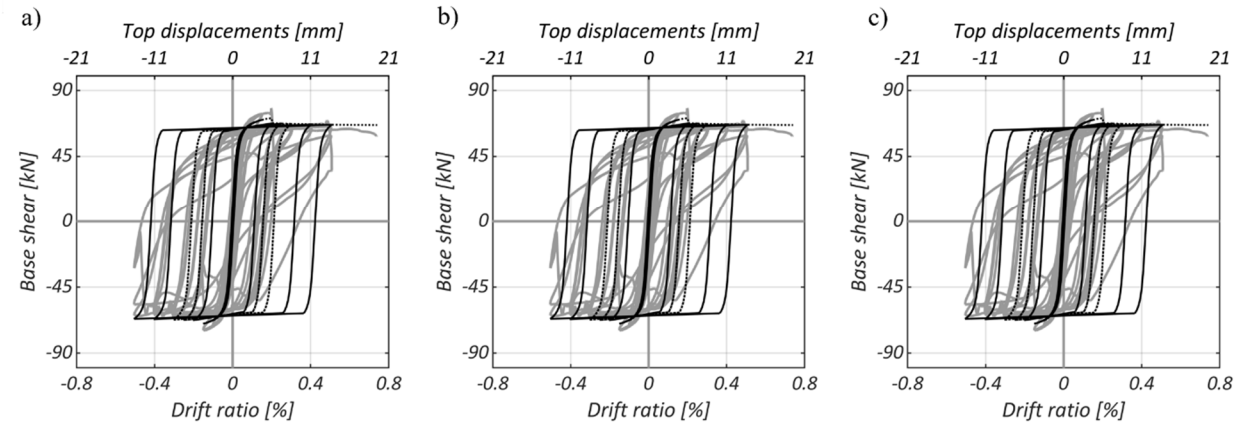

Figure 6: Hysteretic cycles of the bare pier using the (a) Penna et al. [5], (b) Bracchi et al. [6], and (c) multilinear material models. Experimental and numerical responses in gray and black, respectively.

Also the numerical model of the retrofitted pier provides results fairly in-line with the experimental observations (Figure 7). The peak strength is well reproduced by all the constitutive models, resulting in a discrepancy of approximately 2% in all cases. It is worth noting that in the experiment the timber frame prevented the shear-sliding mechanism, allowing the element to reach its maximum flexural strength, with consequent significant toe-crushing at the base. The associated severe damage reduced the effective dimensions of the pier, resulting in lateral strength degradation and in triggering of a diagonal crack at 0.80% drift ratio, which ultimately led to shear failure of the specimen at 2% drift ratio.

The numerical model correctly predicts extensive masonry plasticization, independent of the constitutive law adopted. Due to this plasticization, the choice of masonry material model affects the cyclic response of the retrofitted pier, especially in terms of energy dissipation and strength degradation. In fact, a parallel-elastic unloading branch according to Figure 2b allows to slightly better account for damage accumulation, with consequent increased energy dissipation, compared to the recentering behaviour of the law of Figure 2a. However, the elasto-perfectly plastic plateau limits the accuracy of the formulation. On the other hand, the multilinear model proposed in Figure 2c allows to better simulate the material degradation associated with toe-crushing, showing a progressive reduction of the lateral strength up to reaching the onset of the diagonal crack observed during the experimental test, which ultimately led to shear failure of the specimen. As previously mentioned, this crack results from the reduction in the effective dimensions of the pier due to severe damage, a phenomenon that cannot be fully accounted for through a macroelement model.

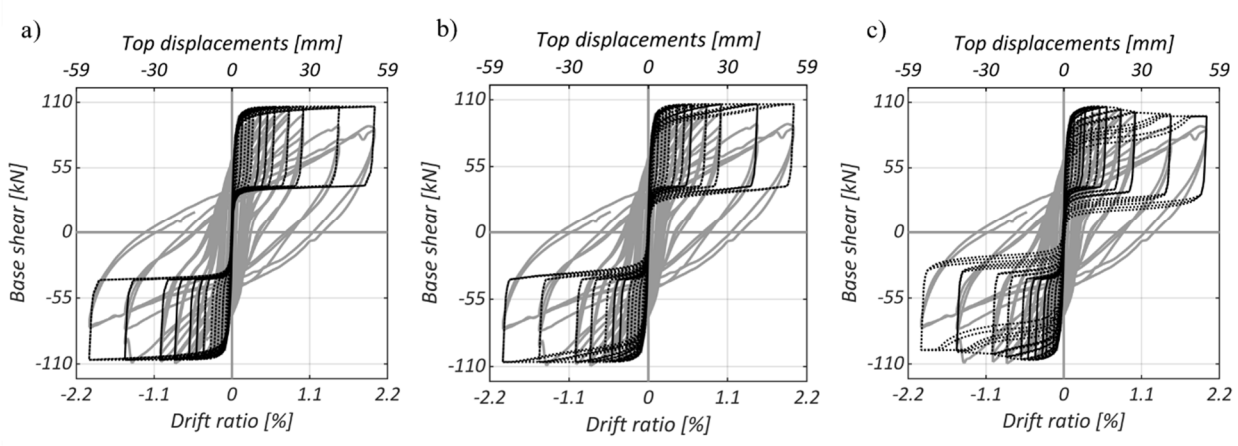

Figure 7: Hysteretic cycles of the retrofitted pier using the (a) Penna et al. [5], (b) Bracchi et al. [6], and (c) multilinear material models. Experimental and numerical responses in gray and black, respectively.

CONCLUSIONS

The growing interest in reducing the seismic vulnerability of unreinforced masonry (URM) structures has led the research community towards the development of efficient, cost-effective and sustainable retrofitting solutions. However, integrating these solutions into numerical models typically requires detailed approaches that need careful calibration and may compromise computational efficiency.

This paper presents a novel three-dimensional equivalent-frame macroelement that enhances the capabilities of the previous well-established two-dimensional formulation. The extension to the three-dimensional space is complemented by the introduction of a mid-height interface that, acting as an additional integration section, allows to reproduce the correct axial-flexural stiffness of a masonry panel regardless of the boundary conditions, thus avoiding manual or iterative adjustments. The macroelement

offers both stripe and full fiber discretization of the interfaces, favoring computational efficiency on the one hand, and constitutive model versatility on the other hand. Furthermore, the bi-axial contribution of strengthening and reinforcement solutions is explicitly modeled by adding analytical stripes or fibers with different mechanical properties to the macroelement interfaces, enforcing a linear deformation profile through kinematic compatibility relationships.

The capabilities of the proposed macroelement are validated against two experimental in-plane quasi-static shear-compression tests on calcium silicate (CS) masonry piers with identical dimensions and mechanical properties. The first pier is modeled in its bare configuration, while the second includes a retrofitting solution consisting of a timber frame and oriented strand boards (OSBs) to enhance flexural and shear strength, respectively. The flexural contribution of the timber frame is explicitly accounted for by modeling the tie-down steel connections as lumped elements with an elastoplastic constitutive law, whereas the shear enhancement provided by the OSB panels is implicitly considered through increased cohesion and friction parameters.

The numerical model of the bare pier shows good agreement with the experimental response, successfully capturing initial stiffness, lateral and residual strength, energy dissipation and failure mechanisms. No influence is obtained from the constitutive law assigned to the masonry material in compression, as the compressive strength of masonry is not reached throughout the displacement history.

The model of the retrofitted pier shows only marginal deviations from the experimental outcomes in terms of lateral strength. However, the constitutive law adopted for the masonry affects the accuracy on the cyclic behavior and residual strength prediction. In fact, even though a parallel-elastic unloading improves the cyclic response, an elasto-perfectly plastic idealization does not allow to follow the actual strength degradation of the material. On the other hand, the multilinear model implemented in the full fiber formulation results in closer prediction of the experimental hysteretic response up to reaching the onset of the diagonal crack on the specimen.

Overall, thanks to its improved formulation, the proposed macroelement proves to be a suitable tool for modeling unstrengthened and strengthened masonry elements, accommodating a wide range of retrofit solutions and allowing different trade-offs between prediction accuracy and computational effort. Future developments will allow to explicitly incorporate also the effect of strengthening and reinforcing materials on the shear behavior. Also, the proposed macroelement will be further validated against experimental results from unreinforced masonry elements strengthened with different solutions, such as CRM or FRCM.

ACKNOWLEDGEMENTS

This study is conducted within the DPC-ReLUIS (2024-2026) Work Package 5 “Integrated and sustainable interventions for existing buildings” and Work Package 10 “Code contributions for existing masonry constructions” funded by the Italian Department of Civil Protection (DPC). The authors would like to thank Nederlandse Aardolie Maatschappij BV (NAM) and the EUCENTRE Foundation, Italy, for funding and coordinating the experimental program. Note that the opinions and conclusions presented by the authors do not necessarily reflect those of the funding entities.

REFERENCES

[1] Papanicolaou, C.G., Triantafillou, T.C., Papathanasiou, M., and Karlos, K. (2008). “Textile reinforced mortar (TRM) versus FRP as strengthening material of URM walls: out-of-plane cyclic loading.” *Mater. Struct.*, 41(1), 143-157.

[2] Valluzzi, M.R., Modena, C., and de Felice, G. (2014). “Current practice and open issues in strengthening historical buildings with composites.” *Mater. Struct.*, 47(12), 1971-1985.

[3] Damiani, N., DeJong, MJ., Albanesi, L., Penna, A., and Morandi, P (2023). "Distinct element modeling of the in-plane response of a steel-framed retrofit solution for URM structures." *Earthquake Engng. Struct. Dyn.*, 52, 3030–3052.
[4] Guerrini, G., N. Damiani, M. Miglietta, and F. Graziotti. (2021). "Cyclic response of masonry piers retrofitted with timber frames and boards." *Proc., Institution of Civil Engineers - Structures and Buildings,* 174 (5), 372–88.
[5] Penna, A., Lagomarsino, S., and Galasco, A. (2014). "A Nonlinear Macroelement Model for the Seismic Analysis of Masonry Buildings." *Earthquake Engng. Struct. Dyn.*, 43(2), 159-179.
[6] Bracchi, S., Galasco, A., and Penna, A. (2021). "A novel macroelement model for the nonlinear analysis of masonry buildings. part 1: axial and flexural behavior." *Earthquake Engng. Struct. Dyn.* 50(8), 2233-2252.
[7] Bracchi, S., and Penna, A. (2021). "A novel macroelement model for the nonlinear analysis of masonry buildings. part 2: shear behavior." *Earthquake Engng. Struct. Dyn.*, 50(8), 2212-2232.
[8] Guerrini, G., Salvatori, C., Senaldi, I. E., and Penna, A. (2021). "Experimental and numerical assessment of seismic retrofit solutions for stone masonry buildings." *Geosciences*, 11(6).
[9] Ministry of Infrastructures and Transport (2018). "Norme Tecniche per le Costruzioni, DM 17/01/2018." *Ministry of Infrastructures and Transport*, Rome, Italy (in Italian).
[10] Ministry of Infrastructures and Transport (2019). "Istruzioni per l'Applicazione dell'Aggiornamento delle "Norme Tecniche per le Costruzioni", Circ. 7 of 21/01/2019." *Ministry of Infrastructures and Transport,* Rome, Italy (in Italian).
[11] Bracchi, S., Rota, M., and Penna, A. (2024). "Modelling reinforced masonry buildings by a mechanics-based macroelement approach." *Earthquake Engng. Struct. Dyn.*, 54, 508–529.
[12] Vanin, F., Penna, A., and Beyer, K. (2020). "A three-dimensional macroelement for modelling the in-plane and out-of-plane response of masonry walls." *Earthquake Engng. Struct. Dyn.*, 49(14), 1365-1387.
[13] Damiani, N., Miglietta, M., Guerrini, G., and Graziotti, F. (2023), "Numerical assessment of the seismic performance of a timber retrofit solution for unreinforced masonry buildings." *Int. J. Archit. Herit.*, 17(1), 114-133.
[14] Gambarotta, L. and Lagomarsino, S. (1997a). "Damage Models for the Seismic Response of Brick Masonry Shear Walls. Part I: The Mortar Joint Model and its Applications." *Earthquake Engng. Struct. Dyn.*, 26(4), 423-439.
[15] Gambarotta, L. and Lagomarsino, S. (1997b). "Damage Models for the Seismic Response of Brick Masonry Shear Walls. Part II: The Continuum Model and its Applications." *Earthquake Engng. Struct. Dyn.*, 26(4), 441-462.
[16] Salvatori, C., Guerrini, G., Galasco, A., and Penna, A. (2025). "A Macroelement Formulation for Modeling Strengthened and Reinforced Masonry Elements." *In: Milani, G., Ghiassi, B. (eds) 18th International Brick and Block Masonry Conference. IB²MaC 2024. Lecture Notes in Civil Engineering,* 613. Springer, Cham.
[17] Graziotti, F., Penna, A., and Magenes, G. (2019). "A comprehensive in situ and laboratory testing programme supporting seismic risk analysis of URM buildings subjected to induced earthquakes." *Bull. Earthquake Eng.*, 17, 4575–4599.
[18] Miglietta, M., Mazzella, L., Grottoli, L., Guerrini, G., and Graziotti, F. (2018). "Full-scale Shaking Table Test on A Dutch URM Cavity-Wall Terraced-House End Unit – EUC-BUILD-6." *Eucentre Foundation*, Pavia, Italy, Research Report EUC160/2018U.
[19] Guerrini, G., Damiani, N., Miglietta, M., and Graziotti, F. (2024). "Experimental validation of analytical equations for retrofitting masonry buildings with timber frames and boards." *Engineering Structures*, 300, 117124.
[20] Damiani, N., Guerrini, G., and Graziotti, F. (2024). "Design procedure for a timber-based seismic retrofit applied to masonry buildings." *Eng. Struct.*, 301, 116991.